

Introduction of effective dielectric constant to the Poisson-Nernst-Planck model

Atsushi Sawada

Performance Materials Advanced Technologies, Merck Ltd., Aikawa, Kanagawa 243-0303, Japan

(Received 18 June 2015; revised manuscript received 2 January 2016; published 19 May 2016)

The Poisson-Nernst-Planck (PNP) model has been widely used for analyzing impedance or dielectric spectra observed for dilute electrolytic cells. In the analysis, the behavior of mobile ions in the cell under an external electric field has been explained by a conductive nature regardless of ionic concentrations. However, if the cell has parallel-plate blocking electrodes, the mobile ions may also play a role as a dielectric medium in the cell by the effect of space-charge polarization when the ionic concentration is sufficiently low. Thus the mobile ions confined between the blocking electrodes can have conductive and dielectric natures simultaneously, and their intensities are affected by the ionic concentration and the adsorption of solvent molecules on the electrodes. The balance of the conductive and dielectric natures is quantitatively determined by introducing an effective dielectric constant to the PNP model in the data analysis. The generalized PNP model with the effective dielectric constant successfully explains the anomalous frequency-dependent dielectric behaviors brought about by the mobile ions in dilute electrolytic cells, for which the conventional PNP model fails in interpretation.

DOI: [10.1103/PhysRevE.93.052608](https://doi.org/10.1103/PhysRevE.93.052608)**I. INTRODUCTION****A. Poisson-Nernst-Planck (PNP) model and Poisson-Boltzmann (PB) model**

Impedance or dielectric spectroscopy is a very powerful diagnostic tool for electrochemical cells and widely used not only for analyzing electrode processes such as polarization and/or reaction but also for determining the bulk properties of electrolytes in the cells [1]. In the data analysis, an appropriate equivalent circuit is usually constructed using several elements such as capacitors and resistors, so that the circuit impedance fits to the measured impedance spectrum in a wide frequency range. Even though one could get good fits, it is sometimes difficult to physically interpret the role of every circuit element. In such cases, the PNP model may help one to acquire deeper understanding about the physical phenomena in the cells induced by external electric fields. The impedance measurement is usually carried out by applying an ac voltage with small amplitude to the cell in order to obtain a linear response in the current. In this sense, the PNP model for a small ac field has been developed intensively in the past [2–5].

If an electrolytic cell has a parallel-plate blocking electrode with no faradic current, it has been believed that electric double layers (EDLs) are constructed at the interfaces between the bulk solution and electrodes by applying an external voltage to the cell. The fundamental theory of EDL was developed by Helmholtz, Gouy-Chapman, Stern, Grahame, etc., and the classical models constructed by them have brought about great success in identifying the EDL structures in electrolytic cells, particularly for aqueous solutions [6,7]. The Gouy-Chapman (GC) theory expresses a diffuse double layer [8,9], and it directly represents the performance of EDL in the absence of true charge at the electrodes [i.e., the state of the potential of zero charge (PZC)]. In the GC theory, the capacitance of the diffuse double layer, C_d , is derived by solving the Poisson-Boltzmann (PB) equation. In the condition of PZC, the value of C_d per unit area is expressed with the dielectric constant of solvent material and an electrode separation of the Debye length L_D .

The PNP equations describe the linear-response dynamics of electrolytes perturbed from equilibrium, whereas the PB

equation represents the distribution of electrolytes in a static field. For electrolytic cells with a parallel-plate blocking electrode, it has been shown that the equivalent parallel capacitance at a low-end frequency predicted by the PNP model becomes approximately equal to the value of C_d , when the electrode separation d is much larger than L_D [4,10]. In general, it has been believed that this relation is valid regardless of the concentration of electrolyte. Is this correct? This question may link to an issue of whether the mobile ions have “conductive” or “dielectric” nature in the electrolytic cell.

B. Dielectric nature of mobile ions

Electric polarization in an atom or molecule is not the only case of dipole formation. When a part is charged negatively and the other part is charged positively by the biased distribution of true charges in a space but the space is electrically neutral as a whole, the polarized space may behave as a dipole from a distant view. If we perform the multipole expansion for a space where the presence of true charges is localized, the charge density ρ is represented by the sum of the charge density ρ_0 that brings about monopole q , the charge density ρ^p that brings about dipole p , the charge density ρ^Q that brings about quadrupole $Q \cdots$, when q , p , $Q \cdots$ are set at origin, and expressed as [11]

$$\rho = \rho_0 + \rho^p + \rho^Q + \cdots = \rho_0 - \nabla \cdot \mathbf{P}^{\text{tot}}. \quad (1)$$

The total polarization density \mathbf{P}^{tot} is the sum of the contributions from all multipoles, and written as

$$\mathbf{P}^{\text{tot}} = \mathbf{P} + \mathbf{P}^Q + \cdots = \mathbf{P} - \nabla \cdot \mathbf{Q}_d + \cdots, \quad (2)$$

where \mathbf{Q}_d is the density of quadrupole moment. The electric flux density \mathbf{D} is expressed as $\mathbf{D} = \epsilon_0 \mathbf{E} + \mathbf{P}$ (ϵ_0 is the dielectric constant of free space, \mathbf{E} is the electric field), and the polarization density \mathbf{P} is usually defined by the dipole moment of bound charge in a molecule. However, \mathbf{P} has to be defined including the contribution of ρ^p if this exists in the space of the problem [11].

Let us consider a redistribution of mobile ions in a dilute electrolytic cell with a parallel-plate blocking electrode under

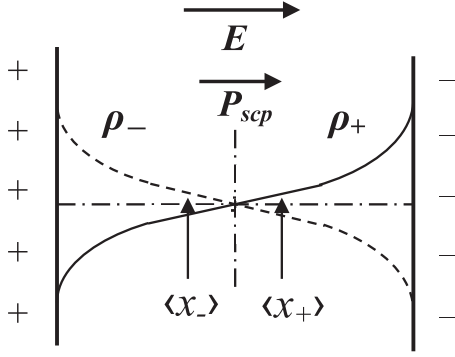


FIG. 1. Schematic representation of ionic distribution under an external field.

the influence of an external field. Here, we assume that a 1:1 type electrolyte is completely dissociated in the cell. Both the positive and negative ions are uniformly distributed in the cell in the absence of the external field, and they redistribute after applying the external field. The mobility and diffusion coefficient of a positive ion is assumed to be equal to those of a negative ion, respectively. In an equilibrium, as shown in Fig. 1, the positive and negative ions may be redistributed exhibiting concentration gradients due to a diffusion effect, and a macroscopic polarization P_{scp} (space-charge polarization) may be generated in the cell.

If the excess ions deposited on the electrode electrically compensate true charges having a countersign, the excess ions are regarded as polarization charges and they induce a polarization, the impact of which is given to a whole space between the electrodes. If an external voltage source is connected to the electrodes, it must supply true charges to the electrodes in order to keep the voltage constant. This is a dielectric effect generated by P_{scp} . The dielectric effect of P_{scp} is similar to that of the usual polarization brought about by the bound charges of molecules. Therefore, the contribution of P_{scp} has to be included in the dielectric constant of Poisson's equation in addition to the molecular polarizations of the solvent in the analysis using the PNP model [12–15]. This treatment for Poisson's equation implies that the space between the electrodes is filled with a continuum dielectric with the dielectric constant determined by P_{scp} . The contribution of P_{scp} to the dielectric constant of Poisson's equation is derived by solving the PNP equations in which Poisson's equation is included. Accordingly, the magnitude of P_{scp} has to be determined self-consistently, and a solution of this problem has been shown in the author's previous work [14]. Barbero *et al.* have given negative comments on this treatment [16–18]; however, they have not made reference to the dielectric nature of mobile ions localized in macroscopic space, that is the fundamental issue of P_{scp} .

Until recently, P_{scp} has been interpreted as just a double layer formation by mobile ions and true charges at the interface between the electrolyte solution and the electrode, and the kinetic phenomenon has been analyzed by using the classical PNP model. The contribution of P_{scp} is not included in the dielectric constant in Poisson's equation in the classical PNP model [4,19–21]. In this case, the deposition of external charges at the electrodes progresses by the displacement of

ions without the dielectric effect of P_{scp} . It turns out that Poisson's equation gives an electric field only between the electrodes and excess ions near the electrodes and denies the generation of an electric field over the bulk layer.

The electric field and the ionic distribution determined by Poisson's equation without the contribution of P_{scp} conform to those predicted by the PB model when the distance between the electrodes is sufficiently large compared with the Debye length L_D . L_D is obtained by solving the PB equation with the boundary condition that the potential becomes zero at infinity. This implies that the total potential difference must appear between the electrode and the excess ions. On the other hand, there is no logical necessity such that the electric field must be generated between the electrode and the excess ions when the potential difference is given to the parallel-plate blocking electrode. Therefore, the electric field generated between the electrodes and the redistributed ions may not be predicted by the PB model.

Let us apply the multipole expansion to the present electrolytic cell as shown in Fig. 1. Here, we consider a one-dimensional model. We find straightforwardly that $\rho_0 = 0$ because the total amount of the negative ions in the cell is equal to that of the positive ions. The polarization density P_{scp} induced by the displacements of the ions per unit volume is expressed as [14,20,21]

$$P_{scp} = ec_0(\langle x_+ \rangle - \langle x_- \rangle) = ec_0s, \quad (3)$$

where e is the elementary charge; c_0 is the number of the positive or negative ions per unit volume in the absence of the external field; $\langle x_+ \rangle$ and $\langle x_- \rangle$ are the average positions of the positive and negative mobile ions, respectively, displaced under an applied external field; and s is the distance between the average positions. Assuming the unit volume ΔV , the redistributed condition of the positive and negative ions is deemed to be equivalent to the case that two point charges, $+Q (= +ec_0\Delta V)$ and $-Q (= -ec_0\Delta V)$, are set in the direction of normal to the electrode surface with an interval s so that the center between the two charges coincides with the center between the electrodes. Applying the multipole expansion to this system by taking an origin at the center between the electrodes and a viewing point with the distance r from the origin ($r \gg s$), we find that the terms with odd powers of r become zero and the terms with even powers are nonzero [22]. This fact results in the quadrupole term becoming zero and only the octupole term and the higher terms with even powers of r remain in the expansion. The value of s is derived by a numerical calculation using the PNP equation [12,14]. Providing that the distance between the electrodes of the cell is 2.26×10^{-5} m, and the voltage applied to the cell is 0.007 V [23], and the number density of ions $c_0 = 1.2 \times 10^{20} \text{ m}^{-3}$ [14], we obtain $s = 8.8 \times 10^{-7}$ m and $s/r = 0.039$, assuming the distance r is equal to half of the electrodes' separation. The ratio of the contributions to the total polarization between the dipole and the octupole terms is expressed as $s/r^2 : (2/r)[s/(2r)]^3$. We obtain that $s/r^2 : (2/r)[s/(2r)]^3 = 1 : 3.8 \times 10^{-4}$. Accordingly, the total polarization in this condition is approximately equal to the polarization induced by the dipole term. This result indicates that the mobile ions work as “polarization charges” in the present condition.

C. Scope of the present work

As described in the previous section, the mobile ions redistributed in the dilute electrolytic cell with blocking electrodes under the influence of an external field should be considered to be macroscopic “bound charges” rather than “free charges.” However, we have to consider two factors that affect the dielectric nature of mobile ions in the electrolytic cell. One is that the amount of mobile ions deposited on the electrodes is restricted for high ionic concentrations. According to the simulation result [13], the cell capacitance brought about by P_{scp} proportionally increases with ionic concentration. However, the capacity of the mobile ions collected at the electrode surface is limited by the distance of the closest approach for ions that is determined by steric effects such as the finite size of the ion [7] and the electronic spillover from the electrode surface [24–26]. The author has introduced a capacitance that represents the limitation, and analyzed the dielectric spectra measured for dilute electrolytic cells by using an equivalent electric circuit including the capacitance [27]. In the previous work, a homogeneous electric field was assumed in the cell for comparably low ionic concentrations, that was not satisfying Poisson’s equation. If the number density of mobile ions becomes so large that the capacitance brought about by the space-charge polarization is comparable or larger than the limited capacitance at the interfaces, the assumption of the homogeneous field will be no longer valid and the electric field will be concentrated near the electrodes. This speculation suggests that the performance of the mobile ions in the cell will change from the dielectric nature to the conductive nature through an inflection point determined by the limited capacitance.

The other factor is that the mobile ions cannot approach the electrode if solvent molecules are adsorbed on the electrodes robustly. If the solvent molecules are adsorbed on the electrode aligning their dipoles, a potential difference is generated between the electrode and the ions approached and thus the ions may not fully compensate the counter true charges. In this work, in order to cope with the two factors, the PNP equations are solved under the boundary condition developed by Macdonald [28,29] and Franceschetti [29], which includes the rate constants of ionic adsorption on electrodes. It has been confirmed that the same electrolytes as used in the present work adsorb on the electrodes of the cell [30]. The adsorption of the electrolytes on the electrode is achieved by replacing the solvent molecules [7]. The boundary condition does not represent the adsorption-desorption property of the solvent molecules; nevertheless, it may enable one to indirectly evaluate the adsorption strength of the solvent molecules by comparing the adsorption-desorption rates of the same electrolyte measured for different solvent materials. In actual measurements using the present electrolyte, the influence of the ionic adsorption on the complex dielectric constant appears in lower-frequency regions than the regions where the dielectric relaxations due to P_{scp} are observed.

The PNP and PB models for the electrolytic cell may be interpreted by the equivalent circuits shown in Fig. 2. In the figure, C_g is the geometrical capacitance containing the contributions of molecular polarizations of solvent material. $C_{pnp}(\omega)$ and $R_{pnp}(\omega)$ are the capacitance and resistance obtained by the PNP model, respectively, and they vary with

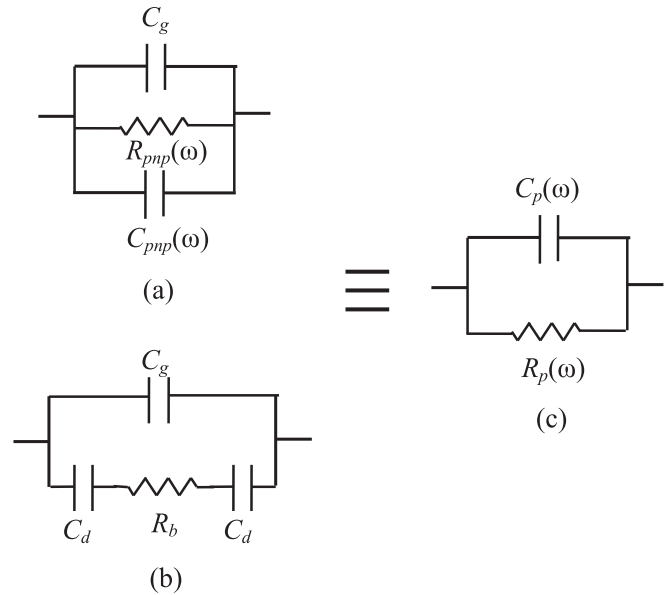


FIG. 2. Equivalent circuits for representing (a) the PNP model, (b) the PB model, and (c) an equivalent parallel circuit for analyzing experimental data.

the frequency of an externally applied ac field. C_d is the capacitance of the diffuse double layer derived by solving the PB equation in the condition of PZC. R_b is the resistance calculated with the conductivity of the bulk layer, which is determined by the mobility and the number density of the mobile ions for a 1:1 electrolyte system. $C_p(\omega)$ and $R_p(\omega)$ are the equivalent parallel capacitance and resistance, respectively, used for analyzing experimental data.

A simulation result obtained by using the equivalent circuits in Fig. 2 for a dilute electrolytic cell is shown in Fig. 3 [13,14]. In the simulation, the electrode separation d is sufficiently

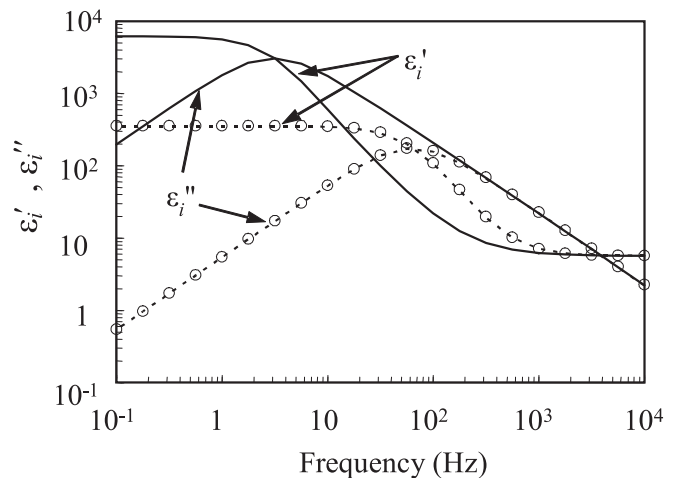


FIG. 3. Frequency dependences of the complex dielectric constant for a dilute electrolytic cell calculated by using the equivalent circuits in Fig. 2. Solid lines represent the values calculated by using the PNP model with the contribution of P_{scp} in the dielectric constant of Poisson’s equation. The dotted lines represent the values by using the PNP model without the contribution of P_{scp} . The open circles represent the values calculated by using the PB model.

larger than L_D . In Fig. 3, the solid lines represent the values of the complex dielectric constant calculated by using the PNP model including the contribution of P_{scp} in the dielectric constant of Poisson's equation, i.e., $\varepsilon = \varepsilon_{\text{solvent}} + \varepsilon_{\text{scp}}$. The dotted lines represent the values by using the PNP model not including the contribution of P_{scp} , i.e., $\varepsilon = \varepsilon_{\text{solvent}}$. The open circles represent the values of the complex dielectric constant calculated by using the PB model. It is found in Fig. 3 that the frequency-dependent curves of the complex dielectric constant, dotted lines, are totally different from those shown by solid lines, but conform to those shown by open circles. This result implies that the PNP model without the contribution of P_{scp} in the dielectric constant of Poisson's equation represents a full conductive nature for the mobile ions, and the dielectric and conductive natures for the mobile ions in the PNP model can be represented by parametrizing the dielectric constant in Poisson's equation.

Since no theoretical model is at present available for analyzing the influence of the adsorbed solvent molecules on charge compensation, the dielectric effect of mobile ions is evaluated by introducing the effective dielectric constant ε_{eff} in the present work that is phenomenologically determined in experiment. ε_{eff} will show how the dielectric effect of mobile ions observed phenomenologically can be interpreted in terms of P_{scp} quantitatively. The frequency dependences of the complex dielectric constant are measured for electrolytic cells with a broader ionic concentration range than that in the previous work [27]. Different polar solvents and electrolytes are used for achieving high values of number density of mobile ions. The observed dielectric spectra are analyzed by using the PNP model with ε_{eff} and the results are discussed in terms of the dielectric and conductive natures for the mobile ions.

II. THEORETICAL EXPRESSIONS OF THE PNP MODEL CONSIDERING IONIC ADSORPTION ON ELECTRODES

Let us consider a parallel-plate cell filled with a 1:1 electrolyte solution. The distance between electrodes is d and the two electrodes are made of the same substance. The electrolyte is completely dissociated and the positive and negative ions are distributed uniformly in the cell at the zero applied potential. There is no true charge on the electrodes in the absence of an external electric field. We restrict our consideration to a one-dimensional case with the transport of the mobile ions in the x direction under an external electric field. Let $p(x,t)$ and $n(x,t)$ be the number densities of the positive and negative ions, respectively, at position x and time t . Considering the experimental system in the present work, we assume that the diffusion coefficient of the positive ion is equal to that of the negative ion; similarly, the mobility of the positive ion is equal to that of the negative ion. Thus, let D and μ be the diffusion coefficient and the mobility of the positive or negative ion, respectively. Under the conditions, the Nernst-Planck equations are expressed as

$$\begin{aligned} \frac{\partial p}{\partial t} &= D \frac{\partial^2 p}{\partial x^2} + \mu \frac{\partial}{\partial x} \left(p \frac{\partial \Phi}{\partial x} \right), \\ \frac{\partial n}{\partial t} &= D \frac{\partial^2 n}{\partial x^2} - \mu \frac{\partial}{\partial x} \left(n \frac{\partial \Phi}{\partial x} \right). \end{aligned} \quad (4)$$

In Eq. (4), we assume that the Einstein relation, $\mu = eD/kT$, is valid. The static potential Φ satisfies Poisson's equation, written as

$$\frac{\partial^2 \Phi}{\partial x^2} = - \frac{e(p-n)}{\varepsilon_0 \varepsilon_r}, \quad (5)$$

where ε_0 is the dielectric constant of free space and ε_r is the relative dielectric constant of solution. The electric field in the cell is expressed as $E = -\partial\Phi/\partial x$.

We discuss the case in which a simple sinusoidal forcing voltage $V(t) = V_1 \exp(i\omega t)$ is applied between the electrodes, where ω is the angular frequency and $i = \sqrt{-1}$. The current through the electrolytic cell will contain all harmonics of the forcing voltage, and accurate solutions for p , n , and E would show that they would all involve zero frequency components with the fundamental and all its overtone. However, the ratio of higher-harmonic components to the fundamental component in p , n , and E may be made negligible by taking V_1 sufficiently small. Thus, by providing such a small V_1 , p , n , E , the current density of positive ion j_p , and the current density of negative ion j_n may all be written in the form [2–5]

$$p(x,t) = p_0 + p_1(x) \exp(i\omega t), \quad (6)$$

where p_0 represents the number density of the positive ion in the absence of the external field. In the present case, the number density of positive ions is equal to that of negative ions in the absence of the external field, and thus we set $p_0 = n_0 = c_0$. Since no dc component is involved in the applied voltage, $E_0 = 0$ and $j_{p0} = j_{n0} = 0$.

We assume that the electrodes of the cell are ideally polarizable and the transport of mobile ions under an external electric field is completely blocked at the electrodes. It has been shown that the specific adsorption of ions to electrodes occurs in electrolytic cells depending on ion species [6,31]. Then we solve the equations given by Eqs. (4)–(6) under the boundary condition developed by Macdonald [28,29] and Franceschetti [29], that represents the process of the ionic adsorption and desorption. In the present model, we assume that the adsorption-desorption rates of the positive ions on the electrode are equal to those of the negative ions. Then the pertinent boundary condition is expressed as

$$\begin{aligned} j_{p1} &= e\mu c_0 E_1 - eD dp_1/dx = -\xi^* e p_1, \quad \text{for } x = -d/2, \\ j_{p1} &= e\mu c_0 E_1 - eD dp_1/dx = \xi^* e p_1, \quad \text{for } x = d/2, \\ j_{n1} &= e\mu c_0 E_1 + eD dn_1/dx = -\xi^* e n_1, \quad \text{for } x = d/2, \\ j_{n1} &= e\mu c_0 E_1 + eD dn_1/dx = \xi^* e n_1, \quad \text{for } x = -d/2. \end{aligned} \quad (7)$$

If no charge transfer occurs between the adsorbed ions and the electrode, ξ^* is written as

$$\xi^* = \xi' + i\xi'' = \frac{\omega^2 \tau^2 \xi_\infty}{1 + \omega^2 \tau^2} + i \frac{\omega \tau \xi_\infty}{1 + \omega^2 \tau^2}. \quad (8)$$

Assuming that the concentration of the positive or negative ions per unit area adsorbed on the electrode is Γ and the net rate of the adsorption of the positive or negative ions is v , it is defined that $\xi_\infty = (\partial v / \partial c_{s1})_\Gamma$, $\tau = -(\partial \Gamma / \partial v)_{c_{s1}}$, where c_{s1} represents the number density of the positive or negative ions at the surface of the electrode [32].

By solving Eqs. (4)–(6) under the boundary condition of Eqs. (7) and (8), the solution for p_1 is expressed as

$$p_1 = \frac{\mu c_0 V_1 \tanh(zx)}{d \left\{ \left[\frac{2}{dz^2 \tau_B} + \xi' + i\xi'' \right] \tanh(zx) - \frac{1}{z\tau_B} + Dz \right\}}, \quad (9)$$

where

$$z = \sqrt{\frac{1 + i\omega\tau_B}{D\tau_B}},$$

and $\tau_B = \varepsilon_0 \varepsilon_r / (2\mu c_0 e)$. The relative dielectric constant ε_r included in τ_B contains two contributions expressed as

$$\varepsilon_r = \varepsilon_{rm} + \varepsilon_{rs}, \quad (10)$$

where ε_{rm} and ε_{rs} stand for the molecular polarizations of the solvent material and the space-charge polarization, respectively. Since the positive and negative ions have the same diffusion coefficient D and mobility μ , it reduces to $p_1(-x) = -p_1(x)$ and $n_1(x) = p_1(-x)$. The current density j_1 becomes

$$j_1 = \varepsilon_0 \varepsilon_{rm} \frac{dE(t)}{dt} + e \left[2\mu c_0 E_1 - D \frac{dp_1}{dx} + D \frac{dn_1}{dx} \right], \quad (11)$$

The total current density J_1 flowing into the electrolyte layer can be obtained by taking a space average of j_1 over the whole layer, and we obtain

$$J_1 = i\omega \varepsilon_0 \varepsilon_{rm} \frac{V_1}{d} + \frac{e}{d} \left\{ 2\mu c_0 V_1 - D \left[p_1 \left(\frac{d}{2} \right) - p_1 \left(-\frac{d}{2} \right) \right] + D \left[n_1 \left(\frac{d}{2} \right) - n_1 \left(-\frac{d}{2} \right) \right] \right\}. \quad (12)$$

The admittance per unit area, $Y_1 (= J_1/V_1)$, is expressed as

$$Y_1 = \frac{i\omega \varepsilon_0 \varepsilon_{rm}}{d} + \frac{2e\mu c_0}{d} - \frac{4e\mu c_0 D}{d^2} \frac{\tanh\left(\frac{zd}{2}\right)}{\left[\frac{2}{dz^2 \tau_B} + \xi' + i\xi'' \right] \tanh\left(\frac{zd}{2}\right) - \frac{1}{z\tau_B} + Dz}. \quad (13)$$

The parallel resistance per unit area, R_p , and the parallel capacitance per unit area, C_p , given by the sum of the space-charge capacitance and the geometrical capacitance are written as $R_p = 1/Y_1'$ and $C_p = Y_1''/\omega$, respectively, providing that $Y_1 = Y_1' + iY_1''$. The parallel circuit with R_p and C_p corresponds to the equivalent circuit (c) in Fig. 2. Thus, we obtain the complex dielectric constant $\varepsilon_i^* = \varepsilon_i' - i\varepsilon_i''$, where

$$\varepsilon_i' = \frac{dC_p}{\varepsilon_0} = \frac{dY_1''}{\omega \varepsilon_0}, \quad (14)$$

$$\varepsilon_i'' = \frac{d}{\omega \varepsilon_0 R_p} = \frac{dY_1'}{\omega \varepsilon_0}. \quad (15)$$

In the present work, the analysis of experimental data is carried out by parametrizing ε_r . In this sense, we replace ε_r by ε_{eff} , that represents the effective dielectric constant. According to Eq. (10), the practical parameter is ε_{rs} .

III. EXPERIMENT

Three kinds of electrolyte solutions (A–C) were prepared.

(A) *Solute: tetrabutylammonium tetraphenylborate (TBATPB), solvent: o-dichlorobenzene (o-DCB)*. The concentrations of TBATPB (Aldrich, purity >99%) in o-DCB (Merck, purity >99%) were 50 ppb (parts per 10⁹), 500 ppb, 5 ppm (parts per 10⁶), and 50 ppm. These concentrations are equal to 1.2×10^{-7} , 1.2×10^{-6} , 1.2×10^{-5} , and 1.2×10^{-4} mol/l, respectively.

(B) *Solute: TBATPB; solvent: dimethylsulphoxyde (DMSO)*. The concentration of TBATPB (Aldrich, purity >99%) doped into DMSO (Aldrich, purity >99%) was 500 ppm. The concentration is equal to 9.8×10^{-4} mol/l.

(C) *Solute: potassium chloride (KCl); solvent: water (H₂O)*. The concentration of KCl (Aldrich, purity >99%) doped into water (ultrapure millipore) was 1.0×10^{-3} mol/l.

The A solutions were injected into parallel-plate glass cells with indium tin oxide (ITO) electrodes, the area and the distance between electrodes of which were 1.13 cm² and 22.2 μ m, respectively. The B solution was injected into the parallel-plate glass cell with ITO electrodes, the area and distance between electrodes of which were 1.13 cm² and 22.6 μ m, respectively. The C solution was injected into the parallel-plate glass cell with gold (Au) electrodes, the area and distance between electrodes of which were 1.13 cm² and 23.5 μ m, respectively.

The impedances of the cells filled with the A solutions were measured using a Solartron 1260 frequency response analyzer (FRA) connected to a 1296 current amplifier in the frequency range between 0.01 Hz and 10 KHz at 20 °C. The impedance of the cell with the B solution was measured using the same apparatus in the frequency range between 0.01 Hz and 1 MHz at 20 °C. The impedance of the cell with the C solution was measured using the same apparatus in the frequency range between 0.01 Hz and 1 MHz at 25 °C. The ac voltage applied to all the cells was 0.005 V (rms). The frequency dependence of the dielectric constant and the dielectric loss factor were calculated from the impedance value observed.

IV. RESULTS AND DISCUSSION

The dielectric spectra observed in measurements are analyzed by using Eqs. (14) and (15) with six fitting parameters. The analytical approach has two objectives: One is to determine the magnitudes of ε_{eff} of the dilute electrolytic solutions when the mobile ions exhibit a dielectric effect, and the other is to investigate major factors which affect the magnitude of ε_{eff} . Two kinds of relaxation phenomena appear in the dielectric spectrum of the electrolytic cell used in the present work. The dielectric relaxation at higher frequencies is attributed to P_{scp} and that at lower frequencies is brought about by the ionic adsorption to the electrodes and the interfacial capacitances limited with the closest approach of ions to the electrodes. The dielectric relaxation at higher frequencies is dominated by three parameters, D , c_0 , and ε_{eff} , while that at lower frequencies is dominated by three parameters, ξ_0 , τ , and the interfacial capacitance C_e [27]. [$C_e/2$ was connected serially to the circuit (c) of Fig. 2 in the data analysis.] Since the different parameters induced different frequency-dependent behaviors on the complex dielectric constant, the six parameters could be determined uniquely in the data fitting process. It was necessary to analyze the dielectric relaxation

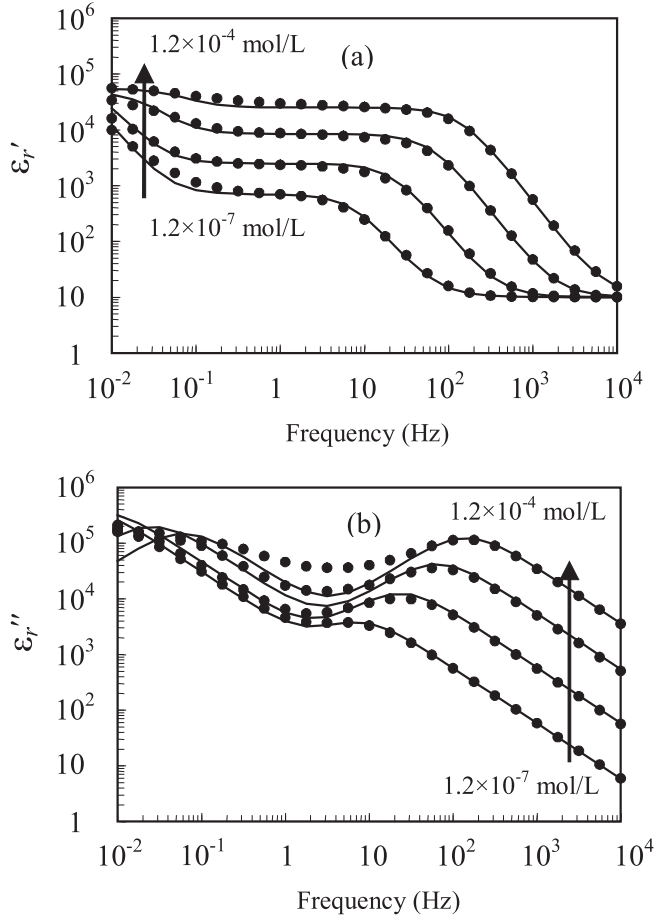


FIG. 4. Frequency dependences of (a) relative dielectric constant ϵ'_r and (b) relative dielectric loss factor ϵ''_r . Filled circles represent observed values for TBATPB-*o*-DCB solutions and solid lines represent calculated values fitted to the observed values.

at lower frequencies in order to investigate the impact of the ionic adsorption on the magnitude of ϵ_{eff} .

In the following sections, we will show the values of the parameters determined by the data analysis and discuss the results in terms of the magnitude of ϵ_{eff} and major factors influencing ϵ_{eff} .

A. Data analysis for the electrolytic cells filled with TBATPB-*o*-DCB solutions

The frequency dependences of ϵ'_r and ϵ''_r for the electrolytic cells filled with the A solutions are shown in in Figs. 4(a) and 4(b), respectively. In the figure, filled circles represent

observed values, and solid lines represent calculated values obtained by means of curve fitting to the observed values. In Fig. 4, good agreements are confirmed between the observed and calculated values in ϵ'_r and ϵ''_r for all the TBATPB concentrations. The values of the parameters determined by the curve fitting are listed in Table I. The frequency-dependent properties of ϵ'_r and ϵ''_r observed in the frequency range over 1 Hz are due to P_{sep} . The value of D is $4.0 \times 10^{-10} \text{ m}^2/\text{s}$ for all the TBATPB concentrations. The Stokes radius of the mobile ions, r_s , is calculated to be $4.05 \times 10^{-10} \text{ m}$ using the Stokes-Einstein equation with the D value and the viscosity value of *o*-DCB. The value of r_s is nearly the same as those obtained by conductometry (TBA+ : $3.8 \times 10^{-10} \text{ m}$, TPB- : $4.1 \times 10^{-10} \text{ m}$) [33,34].

The number density of the ion increases with increasing the doping concentration. In comparison between the doping concentrations and the c_0 values, it is found that over 90% of doped TBATPB is dissociated in the solution when the doping concentration is 1.2×10^{-7} or $1.2 \times 10^{-6} \text{ mol/l}$. For higher doping concentrations, the dissociation ratio gradually decreases. The relative values of ϵ_{eff} is determined to be 60 for the doping concentrations 1.2×10^{-7} and $1.2 \times 10^{-6} \text{ mol/l}$. The value gradually increases with increasing the doping concentration. These values of ϵ_{eff} are much smaller compared to the values calculated assuming the dielectric nature for the mobile ions.

B. Data analysis for the electrolytic cell filled with TBATPB-DMSO solution

The frequency dependences of ϵ'_r and ϵ''_r for the electrolytic cell filled with the B solution are shown in Fig. 5. In the figure, filled and open circles represent observed values for ϵ'_r and ϵ''_r , respectively, and solid and dashed lines represent calculated values obtained by means of curve fitting to the observed values. In Fig. 5, good agreements are confirmed between the observed and calculated values for both ϵ'_r and ϵ''_r . The values of the parameters determined by the curve fitting are listed in Table II. The value of D is $2.9 \times 10^{-10} \text{ m}^2/\text{s}$, and the Stokes radius r_s is calculated to be $3.7 \times 10^{-10} \text{ m}$. In comparison between the doping concentrations and the c_0 values, it is found that almost all the doped TBATPB is dissociated in the solution. The value of ϵ_{eff} is 300. As the value $C_e = 1.0 \times 10^{-5} \text{ F}$ corresponds to the value $\epsilon_{\text{eff}} = 2.3 \times 10^5$, the value of $\epsilon_{\text{eff}} = 300$ is much smaller than the maximum value expected by the dielectric nature for the PNP model.

The electrolyte solution B contains a comparably high amount of mobile ions, and the bulk resistance of the cell is calculated to be around 150Ω from the values of the mobility

TABLE I. Analytical results for electrolytic cells filled with TBATPB-*o*-DCB solutions.

Doped TBATPB concentration		Parameters determined by curve fitting using the equivalent circuit					
(mol/l)	(m^{-3})	D (m^2/s)	c_0 (m^{-3})	ξ_0 (m/s)	τ (s)	C_e (F)	ϵ_{eff}
1.2×10^{-7}	7.0×10^{19}	4.0×10^{-10}	6.5×10^{19}	2.0×10^{-6}	4	1.0×10^{-5}	60
1.2×10^{-6}	7.0×10^{20}	4.0×10^{-10}	6.5×10^{20}	3.0×10^{-7}	10	1.0×10^{-5}	60
1.2×10^{-5}	7.0×10^{21}	4.0×10^{-10}	6.0×10^{21}	8.0×10^{-8}	60	1.0×10^{-5}	80
1.2×10^{-4}	7.0×10^{22}	4.0×10^{-10}	4.0×10^{22}	3.0×10^{-8}	100	1.0×10^{-5}	150

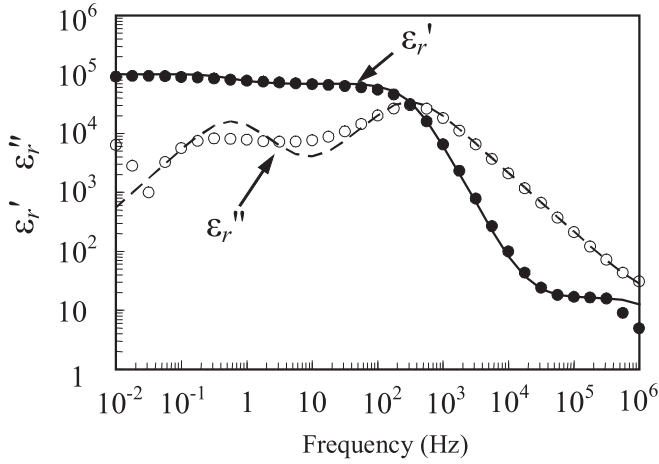


FIG. 5. Frequency dependences of relative dielectric constant ϵ'_r and relative dielectric loss factor ϵ''_r . Filled and open circles represent observed values for TBATPB-DMSO solution. Solid and dashed lines represent calculated values fitted to the observed values.

and number density obtained in Table II. (The mobility value is calculated using the Einstein equation.) Unless the bulk resistance is high enough compared to the electrode resistance, the electrode resistance influences the dielectric spectrum measured in a high-frequency region. In the present case, the influence appeared in the frequency range over 10 kHz due to the comparably high sheet resistance of the ITO electrode. Therefore, the calculation of ϵ'_r and ϵ''_r in Fig. 5 was carried out by using a series resistance R_{ito} that was connected to the main circuit. As a result of the curve fitting, it was obtained that $R_{\text{ito}} = 60 \Omega$.

C. Data analysis for the electrolytic cell filled with KCl aqueous solution

The frequency dependences of ϵ'_r and ϵ''_r for the electrolytic cell filled with the C solution are shown in Fig. 6. In the figure, filled and open circles represent observed values for ϵ'_r and ϵ''_r , respectively, and solid and dashed lines represent calculated values obtained by means of curve fitting to the observed values. The observed values of ϵ'_r drop abruptly once and increase with increasing frequency in the frequency range between 10 and 100 kHz. This phenomenon is considered to be brought about by an inductive factor in the external circuit. The influence of the inductive factor appears in a high-frequency region when the bulk resistance of the cell is not high enough. It is possible to fit the anomalous behavior in ϵ'_r by constructing an appropriate circuit using an inductor and connecting it to the main circuit. Nevertheless, we did not employ such an inductor in the curve fitting process, because it was out of the scope of the problem in the present work.

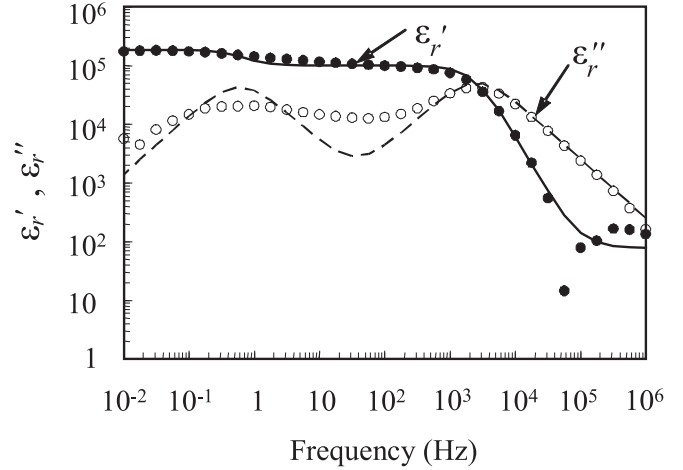


FIG. 6. Frequency dependences of relative dielectric constant, ϵ'_r , and relative dielectric loss factor, ϵ''_r . Filled and open circles represent observed values for a KCl aqueous solution. Solid and dashed lines represent calculated values fitted to the observed values.

The values of the parameters determined by the curve fitting are listed in Table III. The value of D is $1.9 \times 10^{-9} \text{ m}^2/\text{s}$. This value is very close to the value of the diffusion coefficient of mobile ions in KCl aqueous solution shown in Ref. [35]. In comparison between the doping concentrations and the c_0 values, it is found that the doped KCl is completely dissociated in the solution. The value of ϵ_{eff} is 400. As well as the result for the B solution, the value $\epsilon_{\text{eff}} = 400$ is much smaller than the maximum value expected due to the dielectric nature for the PNP model.

D. Data analysis for the electrolytic cells filled with TBATPB-chlorobenzene (CB) solutions

The author has analyzed the frequency-dependent properties of ϵ'_r and ϵ''_r observed for the electrolytic cells filled with TBATPB-CB solutions [27]. In the analysis, the internal electric field of the cell was assumed to be homogeneous. In order to obtain a more accurate analytical result, the data analysis was again performed by using Eqs. (14) and (15) in this work. The result is shown in Fig. 7. The two kinds of dielectric relaxations appear clearly in the figure and the calculated values of ϵ'_r and ϵ''_r fit the observed values quite well. The values of the parameters determined by the curve fitting are listed in Table IV. In Ref. [27], the values of molar concentrations corresponding to the TBATPB doping concentrations, 50 ppb, 500 ppb, 5 ppm, and 50 ppm, were incorrect. The correct values corresponding to the doping concentrations are 9.9×10^{-8} , 9.9×10^{-7} , 9.9×10^{-6} , and $9.9 \times 10^{-5} \text{ mol/l}$, respectively, as shown in Table IV.

TABLE II. Analytical results for an electrolytic cell filled with TBATPB-DMSO solution.

Doped TBATPB concentration		Parameters determined by curve fitting using the equivalent circuit					
(mol/l)	(m^{-3})	D (m^2/s)	c_0 (m^{-3})	ξ_0 (m/s)	τ (s)	C_e (F)	ϵ_{eff}
9.8×10^{-4}	5.9×10^{23}	2.8×10^{-10}	5.9×10^{23}	8.0×10^{-8}	1.0	1.0×10^{-5}	300

TABLE III. Analytical results for an electrolytic cell filled with KCl aqueous solution.

Doped KCl concentration		Parameters determined by curve fitting using the equivalent circuit					
(mol/l)	(m^{-3})	D (m^2/s)	c_0 (m^{-3})	ξ_0 (m/s)	τ (s)	C_e (F)	ε_{eff}
1.0×10^{-3}	6.0×10^{23}	1.9×10^{-9}	6.0×10^{23}	1.5×10^{-7}	10	1.6×10^{-5}	400

The value $D = 6.0 \times 10^{-10} \text{ m}^2/\text{s}$ for the concentration of $9.9 \times 10^{-8} \text{ mol/l}$ leads to $r_s = 4.48 \times 10^{-10} \text{ m}$, and the value $D = 6.8 \times 10^{-10} \text{ m}^2/\text{s}$ for the other concentrations leads to $r_s = 3.95 \times 10^{-10} \text{ m}$. The values of ε_{eff} are much larger than the values shown in Tables I–III, and they increase with the doping concentration from 9.9×10^{-8} to $9.9 \times 10^{-6} \text{ mol/l}$. The large values of ε_{eff} indicate that the mobile ions in the cells have a strong dielectric nature.

E. Estimation of errors in determining the diffusion coefficient in the data analysis

The PNP equations (3) and (4) are derived assuming an ideal solution [35]. By taking the activity of mobile ions into account for an actual solution, the flux of positive ions J_p is

expressed as [35,36]

$$J_p = -D \frac{\partial p}{\partial x} \left(1 + \frac{\partial \ln \gamma}{\partial \ln c_p} \right) - \mu p \frac{\partial \Phi}{\partial x}, \quad (16)$$

where γ is the activity coefficient and c_p is the molar concentration of positive ions. The values of $\partial \ln \gamma / \partial \ln c_p$ were calculated by using the Debye-Hückel (DH) theory. The values of the *o*-DCB solutions were -0.0044 , -0.014 , -0.042 , and -0.107 for the doped TBATPB concentrations 1.2×10^{-7} , 1.2×10^{-6} , 1.2×10^{-5} , and $1.2 \times 10^{-4} \text{ mol/l}$, respectively. The value of the TBATPB-DMSO solution was -0.041 . The value of the KCl aqueous solution was -0.0186 . The values of the CB solutions were -0.007 , -0.016 , -0.033 , and -0.063 for the doped TBATPB concentrations 9.9×10^{-8} , 9.9×10^{-7} , 9.9×10^{-6} , and $9.9 \times 10^{-5} \text{ mol/l}$, respectively. These results indicate that the D values obtained in Tables I–IV contain errors as determined by $\partial \ln \gamma / \partial \ln c_p$.

By applying an external field, the number density of positive or negative ions in a cell increases at one electrode and decreases at the other electrode compared to that at the center position. We calculated the number densities at the electrodes and the center position for the applied voltage of ac 0.005 V (rms) and found that the difference between the number density of the electrode and that of the center was within 6.1% for the TBATPB-*o*-DCB $1.2 \times 10^{-4} \text{ mol/l}$ solution and within 2.3% for the TBATPB-DMSO $9.8 \times 10^{-4} \text{ mol/l}$ solution. Therefore, the finite size of ions does not significantly affect the analytical result obtained in the present study.

The absolute value of $\partial \ln \gamma / \partial \ln c_p$ increases with increasing the concentration of ions assuming the same value of dielectric constant for the solvents. For such high concentrations of ions that the DH theory is not valid, we cannot use Eq. (16) any longer. Recently significant progress on the high-concentration and finite ion-size problems have been made in the field of biophysics [37], such as a new definition of ion-size parameter for determining activity coefficient [38], the introduction of an energy variational method to the PNP model for complex ionic mixture systems considering finite ion-size effects [39], and a new three-dimensional simulation method for diffusing charged and uncharged particles [40].

F. Evaluation of dielectric and conductive nature for mobile ions

The mobile ions in the electrolytic cell with parallel-plate blocking electrodes should intrinsically have a dielectric nature represented by P_{sep} . However, if the number density of ions becomes so high that the contribution of P_{sep} is saturated by the electrode capacitance, the mobile ions may change their main nature from dielectric to conductive. Given the bulk capacitance brought about by P_{sep} , C_b , it is presumed that the value of ε_{eff} increases with increasing c_0 for $C_b \leq C_e/2$ and decreases with increasing c_0 for $C_b > C_e/2$. Here, we assume

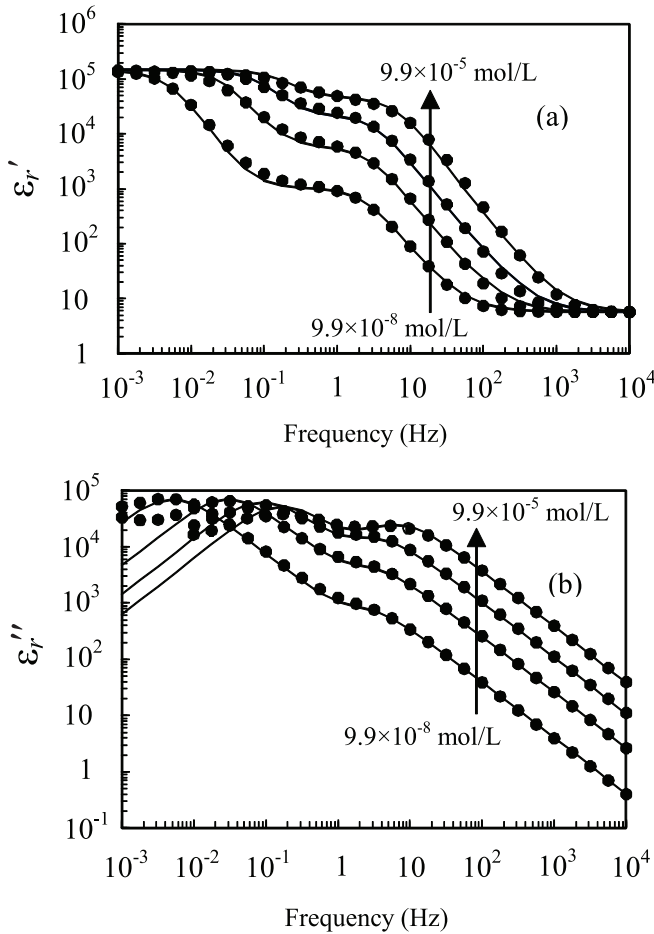


FIG. 7. Frequency dependences of (a) relative dielectric constant ε_r' and (b) relative dielectric loss factor ε_r'' . Filled circles represent observed values for TBATPB-CB solutions and solid lines represent calculated values fitted to the observed values.

TABLE IV. Analytical results for electrolytic cells filled with TBATPB-CB solutions.

Doped TBATPB concentration		Parameters determined by curve fitting using the equivalent circuit					
(mol/l)	(m ⁻³)	D (m ² /s)	c_0 (m ⁻³)	ξ_0 (m/s)	τ (s)	C_e (F)	ε_{eff}
9.9×10^{-8}	5.9×10^{19}	6.0×10^{-10}	3.0×10^{19}	1.2×10^{-5}	1000	1.3×10^{-5}	1800
9.9×10^{-7}	5.9×10^{20}	6.8×10^{-10}	1.7×10^{20}	1.3×10^{-5}	1000	1.3×10^{-5}	9670
9.9×10^{-6}	5.9×10^{21}	6.8×10^{-10}	7.0×10^{20}	1.0×10^{-5}	1000	1.3×10^{-5}	25000
9.9×10^{-5}	5.9×10^{22}	6.8×10^{-10}	2.5×10^{21}	6.0×10^{-6}	1000	1.3×10^{-5}	20000

that $C_b(0)$ stands for the contribution of P_{scp} at a low-end frequency and the value of ε_{eff} is determined by the capacitance ratio between $C_b(0)$ and $C_e/2$.

In the case that the mobile ions have a pure dielectric nature, the relative dielectric constant $\varepsilon_i(\omega)$ calculated under a homogeneous electric field is expressed as [41]

$$\varepsilon_i(\omega) = -\left(\frac{2c_0e^2D}{\omega\varepsilon_0kTG}\right) \left\{ \frac{1 + 2\exp(G)\sin(G) - \exp(2G)}{1 + 2\exp(G)\cos(G) + \exp(2G)} \right\}, \quad (17)$$

where

$$G = d\sqrt{\omega/(2D)}.$$

For $\omega = 0$, we obtain [42]

$$\varepsilon_i(0) = \frac{c_0e^2d^2}{6\varepsilon_0kT}. \quad (18)$$

The value of $C_b(0)$ is calculated to be $C_b(0) = \varepsilon_0\varepsilon_i(0)S/d$, where S is the electrode area. Assuming that the maximum of the effective dielectric constant is $\varepsilon_{\text{eff(max)}}$,

$$\varepsilon_{\text{eff(max)}} = \frac{C_e/2}{C_e/2 + C_b(0)} \varepsilon'_i(0) + \varepsilon_{rm}, \quad \text{for } C_b(0) \leq C_e/2,$$

$$\varepsilon_{\text{eff(max)}} = \frac{C_e/2}{C_e/2 + C_b(0)} \varepsilon_e + \varepsilon_{rm}, \quad \text{for } C_b(0) > C_e/2, \quad (19)$$

where ε_{rm} is the dielectric constant of the solvent and $\varepsilon_e = (C_e/2)d/(\varepsilon_0S)$.

ε_{eff} as a function of the number density of ions is shown in Fig. 8 for each solution: (a) TBATPB in *o*-DCB, (b) TBATPB in DMSO, (c) KCl in water, and (d) TBATPB in CB. In the figure, solid lines represent the calculated values of $\varepsilon_{\text{eff(max)}}$ using Eq. (19). Dashed lines represent the calculated values of $\varepsilon_{\text{eff(min)}}$ ($= \varepsilon_{rm}$), i.e., 9.9 for *o*-DCB, 46.7 for DMSO, 78.3 for water, and 5.7 for CB. Filled circles represent the ε_{eff} values determined by the data analysis shown in Tables I–IV.

In Fig. 8(d), the values of ε_{eff} determined by the data analysis vary along the line of $\varepsilon_{\text{eff(max)}}$ except the value for 9.9×10^{-5} mol/l; this indicates that the TBA+ and TPB− ions in CB exhibit an almost pure dielectric nature in the cells. In Fig. 8(a), the values of ε_{eff} determined by the data analysis vary between $\varepsilon_{\text{eff(max)}}$ and $\varepsilon_{\text{eff(min)}}$, and they are closer to the $\varepsilon_{\text{eff(min)}}$ line. Therefore, the conductive nature is dominant for the TBA+ and TPB− ions in *o*-DCB. This result also shows that the dielectric nature is largely reduced in spite of their comparably small values of the number density. The cause of this phenomenon may be that the *o*-DCB molecules adsorb on

the electrode robustly preventing the approach of TBA+ and TPB− ions.

The parameters of ξ_∞ and τ correspond to the adsorption and desorption constants of ions, respectively, in terms of the Langmuir isotherm [43–45]. Eventually, the larger ξ_∞ , the higher the adsorption rate, and the larger τ , the lower the desorption rate. In comparison between Tables I and IV, the values of ξ_∞ for *o*-DCB are smaller than those for CB in one to three orders of magnitude, and the values of τ for *o*-DCB are also smaller in one to three orders of magnitude. This result implies that it is much more difficult for the TBA+ and TPB− ions in *o*-DCB to be adsorbed on the electrode and much easier to be desorbed than those in CB. The electrical property of the Helmholtz layer is complicated depending on the solvent material. Several factors may affect the formation of the electric field in the Helmholtz layer, such as the dielectric saturation [7,46], the electrostriction [47,48], and the dipole orientation [49]. It is presumed that the electric field in the Helmholtz layer may have an effect of restraining the dielectric effect of P_{scp} . The values of ε_{eff} represented by filled circles in Figs. 8(b) and 8(c) are both not so large but close to the values of $\varepsilon_{\text{eff(max)}}$. These results show that the mobile ions in Figs. 8(b) and 8(c) have conductive dominant natures due to their comparably high ion densities.

If the Debye length is small enough compared to the electrode spacing, the ionic distribution calculated by using the classical PNP model comes to be approximately equal to that calculated by the PB model. Even for the present PNP model, as shown in Fig. 8(b) or 8(c), the ionic distribution calculated with a polar solvent comes to be approximately equal to that by the PB model in the case that $\varepsilon_{\text{eff(max)}} \approx \varepsilon_{\text{eff(min)}}$ for high ionic concentrations such that $c_0 > 10^{25}$ m⁻³. The classical PNP model or the PB model has usually been used for analyzing ionic distributions in electrochemical systems with comparably high ionic concentrations, say, higher than 0.01 mol/l corresponding to $c_0 = 6.022 \times 10^{24}$ m⁻³. Accordingly, the present PNP model does not contradict the great success of the classical PNP model or the PB model in such a high concentration range.

On the other hand, for low concentrations with $\varepsilon_{\text{eff(max)}} \gg \varepsilon_{\text{eff(min)}}$, the ionic distributions predicted by the present PNP model are largely different from those by the PB model. The value of $\varepsilon_{\text{eff(min)}}$ brought about by molecular polarizations of solvent material is independent of the electrode spacing, while the value of $\varepsilon_{\text{eff(max)}}$ becomes large in proportion to the square of the electrode spacing [14]. It becomes that the value of $\varepsilon_{\text{eff(max)}}$ does not physically link to the Debye length. Even though the dielectric constant ($\varepsilon_{\text{eff(min)}}$) in the PB equation is replaced by $\varepsilon_{\text{eff(max)}}$, the ionic distribution predicted by the

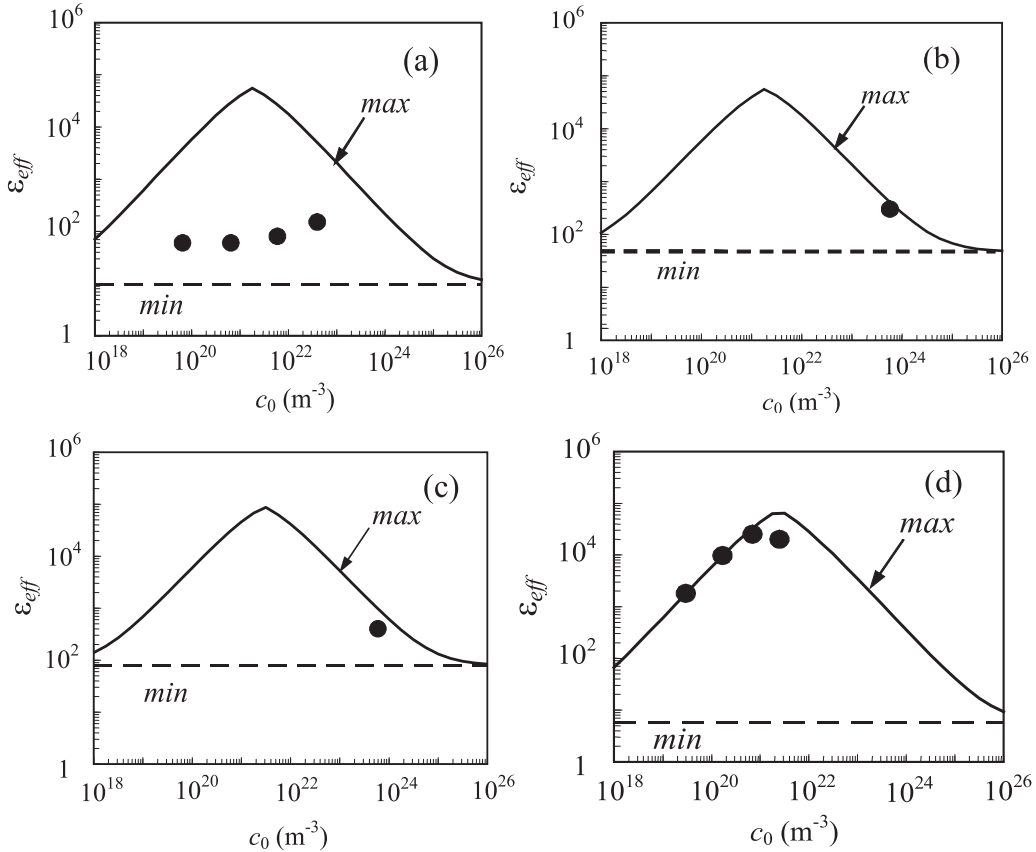


FIG. 8. Effective dielectric constant as a function of ion density of solution: (a) TBATPB in *o*-DCB; (b) TBATPB in DMSO; (c) KCl in water; (d) TBATPB in CB. Solid and dashed lines represent theoretical maximum and minimum values in ϵ_{eff} , respectively. Filled circles represent ϵ_{eff} values determined by the data analysis shown in Tables I–IV.

modified PB model does not fall in line with that by the present PNP model. The value of ϵ_{eff} determined phenomenologically is considered to more or less include the contribution of the space-charge polarization; hence, it should depend on the electrode spacing but not on the Debye length.

V. CONCLUSION

In the data analysis using the PNP model for dielectric spectra observed for dilute electrolytic cells, mobile ions contained in the cells have been considered to be conductive media until recently. However, if the electrolytic cells have parallel-plate blocking electrodes, the mobile ions intrinsically have a dielectric effect represented by P_{scp} . The dielectric nature of the mobile ions is affected by two factors: One is that the amount of mobile ions deposited on the electrodes is restricted for high ionic concentrations, and the other is that the mobile ions cannot approach the electrode when solvent molecules adsorb on the electrodes robustly. Thus, the mobile ions have the conductive and dielectric natures simultaneously in such dilute electrolytic cells. The balance of the dielectric and conductive natures can be determined by introducing ϵ_{eff} to the PNP model. The generalized PNP model with ϵ_{eff} has well explained the anomalous dielectric spectra observed for

dilute electrolytic cells with different ionic concentrations in the range of 10^{-7} to 10^{-3} mol/l.

The introduction of ϵ_{eff} to the PNP model is a phenomenological approach to interpret experimental dielectric spectra; however, the outcome is quite important in terms of the quantitative determination of the dielectric nature for the mobile ions in dielectric. As discussed in Sec. IB, P_{scp} can induce a huge dielectric effect with a small amount of mobile ions owing to the large displacement distance. The dielectric effect is not an imaginal or apparent phenomenon but a pragmatic function to collect true charges. This effect may change the existing concept for developing high- ϵ materials. For instance, the dielectric constants of dielectric substances can be easily increased with the effect of P_{scp} by intentionally doping with mobile charges, and thus an alternative type of supercapacitor may be realized. The present PNP model introduced ϵ_{eff} should be a quite helpful tool, not only for analyzing dilute electrolytic cells but also for designing high- ϵ materials with the concept presented here.

ACKNOWLEDGMENTS

The author is grateful to Prof. S. Naemura of Tottori University and Prof. J. Ross Macdonald of the University of North Carolina for helpful discussion.

- [1] E. Barsoucov and J. R. Macdonald, *Impedance Spectroscopy, Theory, Experiment, and Applications* (J. Wiley & Sons Inc., Hoboken, NJ, 2005).
- [2] G. Jaffe, *Phys. Rev.* **85**, 354 (1952).
- [3] H. Chang and G. Jaffe, *J. Chem. Phys.* **20**, 1071 (1952).
- [4] J. R. Macdonald, *Phys. Rev.* **92**, 4 (1953).
- [5] R. Friauf, *J. Chem. Phys.* **22**, 1329 (1954).
- [6] D. C. Grahame, *Chem. Rev.* **41**, 441 (1947).
- [7] B. E. Conway, *Electrochemical Supercapacitor, Scientific Fundamentals and Technological Applications* (Springer, New York, 1999).
- [8] G. Gouy, *J. Phys. (Paris)* **9**, 457 (1910).
- [9] D. L. Chapman, *Philos. Mag.* **25**, 475 (1913).
- [10] M. Z. Bazant, K. Thornton, and A. Ajdari, *Phys. Rev. E* **70**, 021506 (2004).
- [11] K. Ohta, *Foundations of Classical Electrodynamics* (University of Tokyo Press, Tokyo, 2012), Vol. I (in Japanese).
- [12] A. Sawada, *J. Appl. Phys.* **100**, 074103 (2006).
- [13] A. Sawada, *J. Chem. Phys.* **126**, 224515 (2007).
- [14] A. Sawada, *J. Chem. Phys.* **129**, 064701 (2008).
- [15] A. Sawada, *Phys. Rev. E* **89**, 056402 (2014).
- [16] A. L. Alexe-Ionescu, G. Barbero, and I. Lelidis, *J. Chem. Phys.* **141**, 084505 (2014).
- [17] G. Barbero and I. Lelidis, *J. Appl. Phys.* **115**, 194101 (2014).
- [18] A. L. Alexe-Ionescu, G. Barbero, and I. Lelidis, *Phys. Rev. E* **89**, 056401 (2014).
- [19] F. Stern and C. Weaber, *J. Phys. C* **3**, 1736 (1970).
- [20] S. Uemura, *J. Polym. Sci., Polym. Phys. Ed.* **10**, 2155 (1972).
- [21] R. Coelho, *Rev. Phys. Appl.* **18**, 137 (1983).
- [22] E. M. Purcell and D. J. Morin, *Electricity and Magnetism*, 3rd ed. (Cambridge University Press, New York, 2014).
- [23] The voltage 0.007 V corresponds to the peak voltage of ac 0.005 V (rms) that has been used for experiments.
- [24] J. P. Badiali, M. L. Rosinberg, and J. Goodisman, *J. Electroanal.* **143**, 73 (1983).
- [25] J. P. Badiali, *Electrochim. Acta* **31**, 149 (1986).
- [26] W. Schmickler, *Chem. Rev.* **96**, 3177 (1996).
- [27] A. Sawada, *Phys. Rev. E* **88**, 032406 (2013).
- [28] J. R. Macdonald, *J. Electroanal. Chem.* **70**, 17 (1976).
- [29] D. R. Franceschetti and J. R. Macdonald, *J. Electroanal. Chem.* **82**, 271 (1977).
- [30] A. Sawada, *J. Appl. Phys.* **112**, 044104 (2012).
- [31] M. A. V. Devanathan and M. J. Fernando, *Trans. Faraday Soc.* **58**, 368 (1962).
- [32] R. D. Armstrong and M. Henderson, *J. Electroanal. Chem.* **39**, 81 (1972).
- [33] R. M. Fuoss and E. Hirsch, *J. Am. Chem. Soc.* **82**, 1013 (1960).
- [34] B. S. Krumgalz, *J. Chem. Soc., Faraday Trans. 1* **78**, 437 (1982).
- [35] J. S. Newman and K. E. Thomas-Alyea, *Electrochemical Systems*, 3rd ed. (John Wiley & Sons, New York, 2004).
- [36] L. Tang, *Cem. Concr. Res.* **29**, 1463 (1999).
- [37] B. Eisenberg, *Biophys. J.* **104**, 1849 (2013).
- [38] D. Fraenkel, *Mol. Phys.* **108**, 1435 (2010).
- [39] B. Eisenberg, Y. Hyon, and C. Liu, *J. Chem. Phys.* **133**, 104104 (2010).
- [40] D. Boda and D. Gillespie, *J. Chem. Theory Comput.* **8**, 824 (2012).
- [41] A. Sawada, K. Tarumi, and S. Naemura, *Jpn. J. Appl. Phys., Part 1* **38**, 1418 (1999).
- [42] A. L. Alexe-Ionescu, G. Barbero, and I. Lelidis, *Phys. Rev. E* **80**, 061203 (2009).
- [43] B. Maximus, E. De Ley, A. De Meyere, and H. Pauwels, *Ferroelectrics* **121**, 103 (1991).
- [44] G. Barbero, *Phys. Rev. E* **71**, 062201 (2005).
- [45] L. R. Evangelista, E. K. Lenzi, G. Barbero, and J. R. Macdonald, *J. Chem. Phys.* **138**, 114702 (2013).
- [46] D. C. Grahame, *J. Chem. Phys.* **18**, 903 (1950).
- [47] J. R. Macdonald, *J. Chem. Phys.* **22**, 1857 (1954).
- [48] J. R. Macdonald and C. A. Barlow, *J. Chem. Phys.* **36**, 3062 (1961).
- [49] A. N. Furumkin and B. B. Damaskin, *Electrochim. Acta* **19**, 173 (1974).